行政院國家科學委員會專題研究計畫　成果報告

應變率對奈米複合材料機械行為之影響（II）

計畫類別：個別型計畫
計畫編號：NSC92-2212-E-009-029-
執行期間：92 年 08 月 01 日至 93 年 07 月 31 日
執行單位：國立交通大學機械工程學系

計畫主持人：蔡佳霖

報告類型：精簡報告

處理方式：本計畫可公開查詢

中　華　民　國 93 年 8 月 30 日

行政院國家科學委員會專題研究計畫 成果報告

應變率對奈米複合材料機械行為之影響(II)

計畫類別：個別型計畫
計畫編號：NSC92－2212－E－009－029
執行期間：92 年 08 月 01 日至 93 年 07 月 31 日
執行單位：國立交通大學機械工程學系

計畫主持人：蔡佳霖
計畫參與人員：黃仁傑　王漢偉　郭濬清

成果報告類型：精簡報告

處理方式：本計畫可公開查詢

中　華　民　國 93 年 09 月 02 日

行政院國家科學委員會專題研究計畫成果報告

應變率對奈米複合材料機械行為之影響(II)

計畫編號：NSC 92-2212-E-009-029
執行期限：92 年 08 月 01 日至 93 年 7 月 31 日

主持人：蔡佳霖　國立交通大學機械工程學系
計畫參與人員：黃仁傑
王漢偉
郭濬清

中文摘要

本報告主要研究應變率對尼龍 6 奈米黏土複合材料機械行為的影響。乾與濕的奈米複材試片將在本研究中一併做探討。為了解應變率的影響，添加 5%有機黏土的尼龍 6 奈米複材，將以不同的應變率做測試。應變率小於 1/s 的實驗，係藉由液壓萬能材料試驗機進行量測。而在高應變率下，實驗則將利用分離式霍普金森桿(SHPB)來測試。由實驗結果觀察，乾尼龍 6 奈米複材試片的楊氏係數並不受到應變率的影響。另一方面，在濕試片中，應力應變曲線幾乎呈現非線性的趨勢，而且應變硬化的現象也隨著應變率增加而更加明顯. 比較純尼龍 6 與尼龍 6 奈米複合材料, 我們發現在乾的尼龍 6 試片中, 添加 5% 奈米黏土，楊氏係數則提昇了 32%。此外，在濕的尼龍 6 試片中，其楊氏係數則可以增強到 50%。

關鍵詞：分離式霍普金森桿、奈米複合材料、有機黏土、應變率

Abstract

This research aims to investigate the rate dependent behavior of nylon 6/clay nanocomposites. Both dry and wet nylon 6/clay nanocomposites were examined in this study. To determine the strain rate effect, the nylon 6 nanocomposites with 5 wt% loading of the organoclay were tested at different strain rates. For strain rates less than 1/s, the experiment was conducted using hydraulic MTS machine. However, higher strain rate tests were performed using a Split Hopkinson Pressure Bar (SHPB). Experimental observations reveal that for dry nanocomposites, the Young's modulus is not affected substantially by the strain rates. On the other hand, for the wet nanocomposites, the stress and strain curves are almost nonlinear and become strain hardening when the strain rate increases. Comparison of nylon6/clay nanocomposites and unfilled nylon 6 indicated that the supplement of 5 wt% organoclay in the dry nylon 6 can enhance the Young's modulus to 32%. Moreover, for the wet nylon reinforced with organoclay, the increment of Young's modulus can be achieved by 50%.

Keywords: Split Hopkinson Pressure Bar, nanocomposites, organoclay, strain rate

1. **Introduction**

With the latest development of nanotechnology, composites reinforced with nanoclay platelets have been of great interest to many researchers [1]. The nanoclay platelet is an ultra thin (1 nm) silicate film with lateral dimensions up to 1 μ m. Without special processing, the platelets are held together by the weak ionic bond into clay tactoids. Through the ion exchange process, the sodium ions attracted on the surfaces of the platelets were replaced with organic cations which can improve the interfacial adhesion between the polymer

and the platelet. After an appropriate process, the aggregated platelets can be exfoliated and dispersed uniformly in the polymer. Depending on the degree of the exfoliation, there are three categories of nanocomposites generated, i.e., tactoid, intercalated and exfoliated [2]. Toyota research center carried out a pioneering work on synthesizing the nylon 6/clay nanocomposites by means of polymerization process. The increments of tensile strength, modulus and heat distortion temperature relative to pure resin were reported in their studies [3-5]. Cho *et al* [6] demonstrated the preparation of nylon 6/organoclay nanocomposites via direct melt compounding approach using a conventional twin screw extruder. The mechanical properties and morphology of these nanocomposites were examined and compared to those made by an in situ polymerization process. They concluded that the organoclay was better exfoliated into nylon 6 matrix when compounded using the twin screw extruder rather than the single screw extruder. The similar process for the fabrication of nanocomposites using a twin screw extruder was employed by Liu *et al* [7]. It was indicated that the nanocomposites are superior to nylon 6 in terms of strength and modulus. In view of the foregoing, most of efforts were made to synthesize the nanocomposites as well as to investigate the associated behaviors under quasi-static loading.

It is well known that polymer materials exhibit strain rate sensitivity [8, 9] and thus, the polymer-based nanocomposites could also be affected by strain rate. The high strain responses of polymeric materials were characterized by Chen *et al* [8] using the aluminum split Hopkinson pressure bar (SHPB). A variety of polymers at different strain rates were examined by Walley *et al* [9]. Nevertheless, few literatures concerning the dynamic responses of organoclay nanocomposites were reported. In this study, the dynamic responses of nylon 6/clay nanocomposites were investigated using a SHPB. In order to attain more accurate stress-strain curves, the pulse shaper technique was employed in SHPB tests. Based on the experimental data, the Young's modulus of the materials at high strain rates was evaluated and the results were compared with those measured from lower strain tests. For comparison purpose, unfilled nylon 6 was tested in the same manner and the effect of the organoclay on the mechanical responses of nylon 6 would be discussed.

2. Specimen preparation

The nylon 6/clay nanocomposites (RTP 299AX) and unfilled nylon 6 (RTP 200A) in the form of pellets were commercially available from RTP Company USA. According to the information provided by manufacturer, the nanocomposite pellets containing 5.0 wt% organoclay was prepared via melt compounding process [10]. Both unfilled nylon 6 and nylon 6/clay nanocomposite pellets were dried in vacuum oven at 90 °C for 8hr to eliminate the possible moisture content and then injection molded into cylindrical specimens with 10 mm long and 10 mm in diameter for the compression tests. The barrel temperatures in the injection molding machine were 245, 260, and 255 °C from hopper to die, and the mold temperature was 120 °C . The injection pressure and the holding pressure were 11.27MPa and 13.72MPa, respectively. Prior to tests, all specimens were examined using a microscope to avoid any potential defects, such as voids, existing.

In order to reduce the contact friction between the specimen and the loading fixture, all specimens were polished using a lapping machine with 25 μm aluminum oxide powder. Since nylon6 is hygroscopic as well as nylon6/clay nanocomposites and the mechanical behaviors are affected dramatically by the moisture contents, all specimens considered in this study were divided into two conditions, i.e. dry condition and wet condition. For dry condition, all specimens were kept in a

vacuum oven at temperature 50 °C to prevent from moisture absorption. However, for wet condition, the specimens were immersed into 45℃ water to accelerate the moisture absorption rate for 20 days. The moisture content (%wt) was recorded daily and the results were shown in Figure 1. It was shown that, when the moisture contents were almost saturated, unfilled nylon 6 specimens contained more water than the nylon 6/clay nanocomposites specimens, which illustrates that the presence of organoclay retards water absorption capacity of the nylon 6.

The degree of exfoliation and dispersion of the organoclay in the nanocomposites was evaluated by X-Ray Diffraction (XRD) and Transmission Electron Microscope (TEM). For XRD examination, the neat nylon 6 and nylon 6/clay nanocomposites films with 0.8 mm thickness and 10 mm in diameter were fabricated from the cylindrical specimen using precision section saw. XRD measurement was conducted using a BEDE D1 diffractometer with X-ray wavelength of 1.54Å at a scanning rate of 0.08° /sec from 0.3°~8°. Figure 2 demonstrates the XRD patterns of the nylon 6/clay nanocomposites and the pure nylon 6 from which the d-spacing of the clay platelets in the nanocomposites was estimated as around 90.5Å. Samples with 100 nm thick for TEM analysis were prepared by using a microtome at cryogenic conditions. TEM observations of nylon 6/clay nanocomposites were carried out by a JEOL 200CX with an acceleration voltage of 120KV. The micrographs with 100,000 and 50,000 magnifications were illustrated, respectively, in Figure 3. As shown in the figure, most of the platelets in the form of intercalated clusters are distributed in the matrix and the interlayer spacing is around 7-9 nm which is compatible with the XRD results. Moreover, there are some layers of platelets locally exfoliated and dispersed randomly in the sample. As a result, the material investigated in this study is a combination of intercalated and partially exfoliated nanocomposites.

3. Experimental procedure

In order to investigate the strain rate effect, nylon6/clay nanocomposites were tested in compression at various strain rates. High strain rate experiments were conducted using SHPB. However, low strain rate tests were carried out on hydraulic MTS machine.

(1) High strain rate test

High strain rate compression tests were performed on nylon 6 and nylon 6/clay nanocomposites using a Split Hopkinson Pressure Bar (SHPB) which is an effective but costless apparatus for establishing the dynamic constitutive relations [11]. Figure 4 demonstrate a typical two-gage configuration of a split Hopkinson pressure bar where gage A measures both the incident and reflected pulses in the incident bar, while gage B measures the transmitted pulse. At each of the locations, a pair of diametrically opposed gages were mounted to compensate the bending effect resulted from eccentric impact of the strike bar on the incident bar. During the tests, the strain-gaged cylindrical specimen was sandwiched between the incident bar and the transmission bar. While the impact pulse propagates along the pressure bars and the specimens, the corresponding strain signals measured from the gages were converted into voltages signals by Wheatstone bridge circuits and then amplified using conditioning amplifier. The signals finally were recorded by the digital oscilloscope with sampling rate of 10MHz.

It is noted there are two different bar systems, i.e. steel bar and aluminum alloy (6061-T6) bar, employed for high strain rate tests. The selection of the bar system is based on the relative magnitudes of the pulse signals propagating on the transmission bar and the surrounding noise. For dry nylon6 and nylon6/clay samples, since the

amplitudes of the gage signals on the steel transmission bars are high enough to be recognized, the high strain rate experiment was carried out using steel SPHB. On the other hand, for the wet specimens with lower mechanical impedances, the transmitted gage signals on the steel bars are so weak that the noise prevent from the proper interpretation of the measured signals. Therefore, to effectively enhance the amplitude of the gage signals on the bars, an aluminum alloy SHPB [8] with the characteristic of lower stiffness was adopted instead of steel SHPB for testing the wet samples. In steel bar system, the length of the striker bar is about 90 mm, and the incident bar and the transmission bar were 910 mm and 560 mm long, respectively. Whereas, for aluminum bar system, the lengths of the striker bar, the incident bar and the transmission bar were 40mm, 1170mm and 590mm, respectively. Both of the apparatuses have the same diameter of 13.3 mm. A pulse shaper technique was utilized to produce a gently rising loading pulse which would facilitate the stress equilibrium and homogeneous deformation of the specimens during the strain rate tests. As a result, reliable stress and strain curves, especially in the small strain range, can be extracted from the SHPB tests [12, 13]. This pulse shaping can be achieved using a piece of soft material inserted between the striker bar and the incident bar. In this study, 3 mm thick copper and 5mm thick nylon 6 disks were selected as a pulse shaper for steel and aluminum bar systems, respectively.

Figure 5 shows the typical strain gage signals measured from the incident and transmission bars and the specimen, respectively for dry nylon6/clay nanocomposites. The excitation voltages of the Wheatstone bridge circuits for the gages on the bar and for the specimen gage were 5V and 3V, respectively, and the corresponding amplification was set to be 1000 for the gages on the bars and to be 25 for the specimen gage. By using the Hopkinson bar theory [11], the contact stress P_1 between the incident bar and the specimen, and P_2, the contact stress between the specimen and the transmission bar, can be extracted from the recorded pulse data. The contact stresses P_1 and P_2 for the dry nylon6/clay nanocomposite specimen was shown in Figure 6. It is noted that P1 and P2 almost coincide with each other except that P_1 exhibits greater oscillations than P_2. In view of this, we took P_2 to calculate the compressive stress in the specimen to generate the dynamic stress-strain curve.

Conventionally, the strain history of the specimen during loading can also be calculated using the Hopkinson bar formula with expressions of displacements at the ends of the bars derived from the strain responses recorded at gage A and gage B [11]. In the present study, the strain response of the specimen was also measured using strain gage directly mounted on the specimen. Figure 7 shows the comparison of the strain histories for the nanocomposite specimen obtained using the Hopkinson bar formula and the strain gage directly mounted on the specimen, respectively. It is evident that the strain history calculated based on the Hopkinson bar theory deviates from that directly measured on the specimen. In this study, the strain history measured directly from the specimen was adopted for the determination of the strain rate and for the generation of the dynamic stress-strain curves as well. The average strain rate measured in the steel SHPB tests was 800/s. In the same manner, the high strain rate experiments were performed on the wet specimens using an Aluminum alloy SHPB. The stress curves was calculated from the gage signal on the transmission bar and the corresponding strain curve was obtained from the strain gage adhered on the specimen. The average strain rate in the aluminum SHPB test was around 500/s.

(2) Low strain rate test

For the purpose of the comparison with high strain rates, the nylon6 and nylon6/clay nanocomposites were also tested in compression at lower strain rates using

hydraulic MTS machine. The uniaxial compressive loading was applied on the cylindrical specimens through the end contact surfaces as shown in Figure 8. To have consistency, the samples used for the low strain rate tests were the same as those in the SHPB tests. A self-adjusting device as shown in Figure 8 was applied to eliminate potential bending moments and also to ensure the specimen to be in full contact with the loading surfaces. During the tests, the contact surfaces of the specimens and the loading fixture were lubricated to reduce the contact friction.

Two different nominal strain rates of 0.0001/s and 0.1/s were performed at stroke control mode. The nominal strain rate was the stroke rate of the loading frame divided by the original specimen length. The corresponding true strain rates were measured by using strain gages directly mounted on the specimens. The applied load, displacement and gage signals for each test were recorded using LabView. Figure 9 shows the nominal strain curve and the true strain curve for a dry nylon6/clay specimen tested at the nominal strain rate of 0.0001/s. It is evident that the true strain is quite different from the nominal strain and thus the true strain rate is also different from the nominal strain rate. This discrepancy could be ascribed to the use of the self-adjusting device shown in Figure 8 for the compression test. In this study, the true strain curve was adopted for the generation of the stress and strain curves and also for the calculation of the axial strain rate. Based on the experimental stress and strain curves, the Young's modulus of the materials were determined.

4. Results and discussion

(1) Strain rate effect

The stress and strain curves for dry nylon 6/clay nanocomposites at strain rate ranges from 8×10^{-5}/s to 800/s were shown in Figures 10. The constitutive relations exhibit an apparently linear elastic range followed by a nearly perfect plastic behavior. It was shown that the slopes of the linear portions are almost the same within the tested strain rate ranges indicating that the Young's modulus of the dry nanocomposites is not affected apparently by the strain rates. The measured Young's modulus is around 4.1 GPa. However, the linear elastic ranges increase when the strain rate increases. Figure 11 illustrates the stress and strain curves of wet nylon6/clay nanocomposites at three different strain rates, 8×10^{-5} /s, 8×10^{-2}/s and 500/s. It is noted that for the wet samples, the constitutive curves are almost nonlinear except at strain rate of 500/s and therefore, it is a challenging task to determine the corresponding Young's modulus based on the experimental data. In this study, for the strain rates of 8×10^{-5} /s and 8×10^{-2} /s, the Young's modulus was obtained based on the experimental data with strain range to 0.2% by a linear curve-fitting. Figure 12 illustrates the constitutive relations of wet nylon6/clay nanocomposites together with a linear function. On the other hand, for the high strain rate tests, since the initial portion of the stress and strain curve is little fluctuated, the young's modulus was evaluated by adopting the experimental data with strain level up to 0.5%. Again, a linear function was employed to fit these experimental data and the results were shown in Figure 13. Apparently, with the presence of moisture, the stiffness was dramatically reduced and moreover, the Young's modulus of the material becomes sensitive to the strain rates.

(2) Clay effect

In order to examine the effect of organoclay on the mechanical responses of the nylon6 nanocomposites, the unfilled nylon 6 was also tested in the same manner. Figure 14 demonstrate the stress and strain curves for unfilled dry nylon6 at various strain rates. The constitutive behaviors of unfilled nylon 6 are quite similar to those in dry nylon6/clay nanocomposites except that

the young's modulus is lower with the value of 3.1 GPa. Comparison the results with dry nylon6/clay nanocomposites reveals that the supplement of 5 wt% organoclay in the dry nylon 6 can enhance the Young's modulus up to 32%. The unfilled wet nylon6 samples was illustrated in Figure 15 and again, the Young's modulus was determined by curve-fitting the experimental data at the small strain ranges using a linear function. The results were summarized in Table I together with those obtained from wet nylon6/clay nanocomposites. It was noted that in both unfilled nylon6 and nylon/clay nanocomposites, the moisture contents are different, in other words, the nylon6 possesses higher water absorption capacity than nylon6/clay nanocomposites. As a result, the addition of the organoclay not only retards the moisture absorption but also enhances the stiffness of the wet nylon6 samples. From the comparison, the enhancement of the Young's modulus in the wet samples can be achieved up to 50%.

5. Summary

The following conclusions have been obtained from the present study in the effect of strain rate on mechanical behaviors of nylon 6/clay nanocomposites

- For dry nylon6/clay nanocomposites, the Young's modulus is not affected significantly by strain rate at the strain rate up to 800/s. However, the linear elastic limit increases when the strain rate increases.
- For wet nylon6/clay nanocomposites, the constitutive curves are almost nonlinear and the Young's modulus increases along with the increase of strain rate. In addition, moisture content apparently reduces the stiffness of nylon6/clay nanocomposites.
- The supplement of 5 wt% organoclay in the dry nylon 6 can enhance the Young's modulus to 32 % within the tested strain rate ranges. Moreover, the enhancement can be up to 50% in the wet nylon 6 samples.

6. References

1. Pinnavaia, T.J. and G.W. Beall. 2000, *Polymer-Clay Nanocomposites*, John Wiley & Sons Ltd, New York.
2. Dennis, H.R., D.L. Hunter, D. Chang, S. Kim, J.L. White, J.W. Cho, and D.R. Paul. 2001 "Effect of Melt Processing Conditions on the Extent of Exfoliation in Organoclay-Based Nanocomposites," *Polymer*, Vol. 42, pp. 9513-9522.
3. Usuki, A., Y. Kojima, M. Kawasumi, A. Okada, Y. Fukushima, T. Kurauchi, and O. Kamigaito. 1993 "Synthesis of Nylon 6-Clay Hybrid," *Journal of Materials Research*, Vol. 8, No. 5, pp. 1179-1184.
4. Kojima, Y., A. Usuki, M. Kawasumi, A. Okada, T. Kurauchi, O. Kamigaito, and K. Kaji. 1994 "Fine Structure of Nylon 6-Clay Hybrid," *Journal of Polymer Science: Part B: Polymer Physics*, Vol. 32, pp. 625-630.
5. Usuki, A., A. Koiwai, Y. Kojima, M. Kawasumi, A. Okada, T. Kurauchi, and O. Kamigaito. 1995 "Interaction of Nylon 6-Clay Surface and Mechanical Properties of Nylon 6-Clay Hybrid," *Journal of Applied Polymer Science*, Vol. 55, pp. 119-123.
6. Cho, J.W. and D.R. Paul. 2001 "Nylon 6 Nanocomposites by Melt Compounding," *Polymer*, Vol. 42, pp. 1083-1094.
7. Liu, L., Z. Qi, and X. Zhu. 1999 "Studies on Nylon 6/ Clay Nanocomposites by Melt-Intercalation Process" *Journal of Applied Polymer Science*, Vol. 71, PP. 1133-1138.
8. Chen, W., F. Lu, and M. Cheng. 2002 "Tension and Compression Tests of Two Polymers under Quasi-Static and Dynamic Loading" *Polymer Testing,* Vol. 21, pp. 113-121.
9. Walley, S. M., J. E. Field, P. H. Pope, and N. A. Safford. 1989 "A Study of the Rapid Deformation Behavior of a Range of Polymer," *Philosophical transactions*

of the Royal Society of London A, Vol. 328, pp. 1-33.
10. RTP® material data sheet.
11. Graff, K. F., 1975. *Wave Motion in Elastic Solids.* Dover Publications, New York.
12. Ninan, L., J. Tsai, and C. T. Sun. 2001. "Use of split Hopkinson pressure bar for testing off-axis composites", *International Journal of Impact Engineering,* Vol. 25, pp. 291-313.
13. Chen, W., B. Song, D.J. Frew, and M.J. Forrestal. 2003 "Dynamic Small Strain Measurement of a Metal Specimen with a Split Hopkinson Pressure bar" *Experimental Mechanics*, Vol. 43, No. 1 pp. 20-23.

TABLE I. Young's modulus of wet nylon 6 and nylon 6/clay nanocomposites at different strain rates

Material	High (500/s)	Intermediate (8×10^{-2}/s)	Low (8×10^{-5}/s)
Nylon 6 (moisture)	1.2GPa (8.27%)	1.0GPa (8.52%)	0.7GPa (8.49%)
Nylon 6/clay (moisture)	1.6GPa (7.48%)	1.24GPa (7.64%)	1.06GPa (7.65%)
Enhance ratio	33%	24%	51%

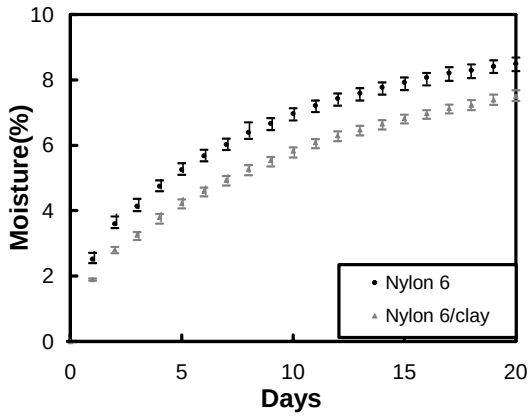

Figure 1. The moisture content of wet nylon 6 and wet nylon 6/clay nanocomposites.

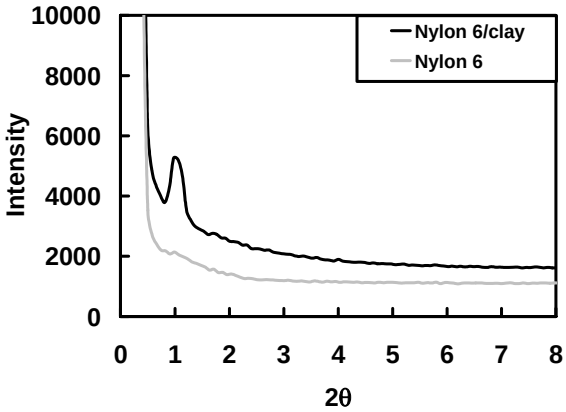

Figure 2. X-ray diffraction patterns for neat nylon 6 and nylon 6/clay nanocomposites

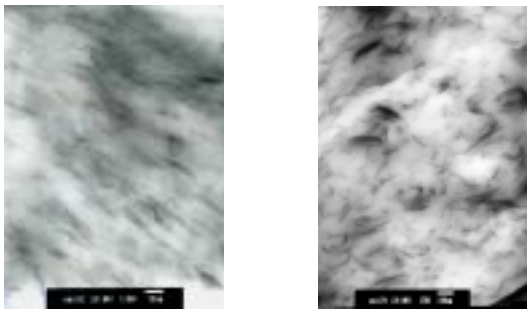

(a) 100000 (b) 50000

Figure 3. TEM micrographs of nylon 6/clay nanocomposites.

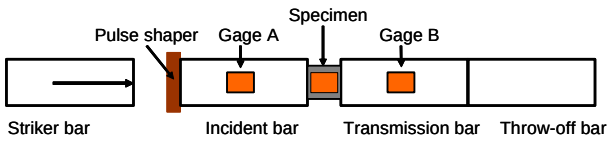

Figure 4. The split Hopkinson pressure bar apparatus.

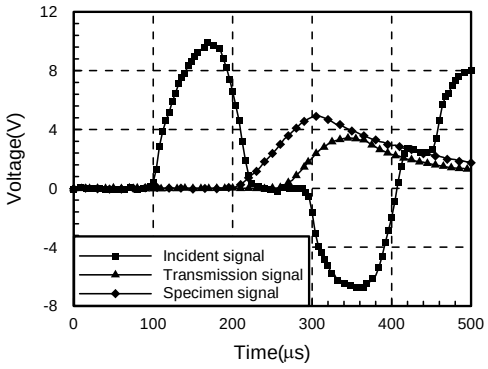

Figure 5. Strain gage signals recorded in SHPB test for dry nylon6/clay nanocomposites.

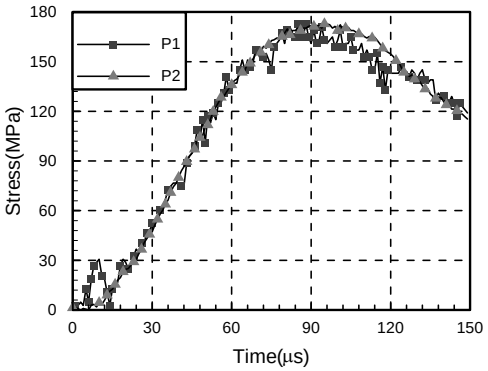

Figure 6. Time histories of the contact stresses for dry nylon6/clay nanocomposites in SHPB tests.

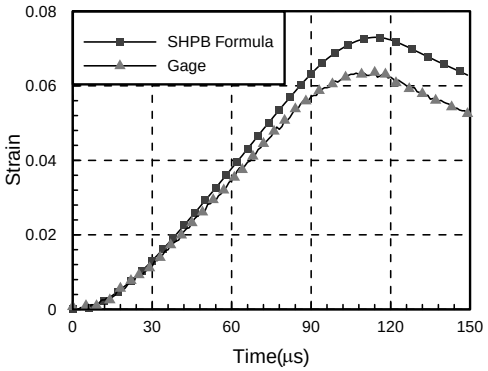

Figure 7. Strain history obtained from Hopkinson bar formula and strain gage signals for dry nylon6/clay nanocomposites in SHPB tests.

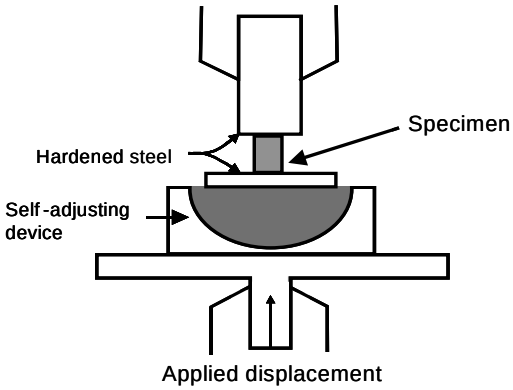

Figure 8. Apparatus for low strain rate tests.

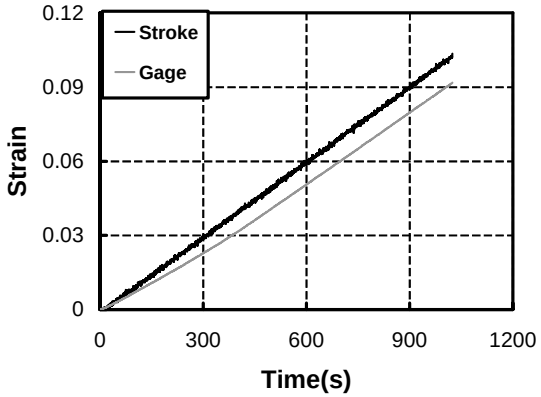

Figure 9. Strain history obtained from stroke and strain gage for dry nylon6/clay nanocomposites at nominal strain rate of 0.0001/s.

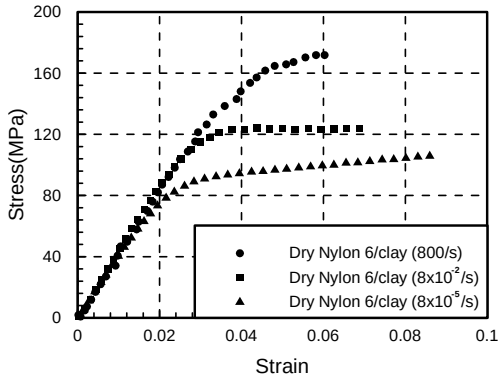

Figure 10. Stress and strain curves of dry nylon 6/clay nanocomposites at three different strain rates.

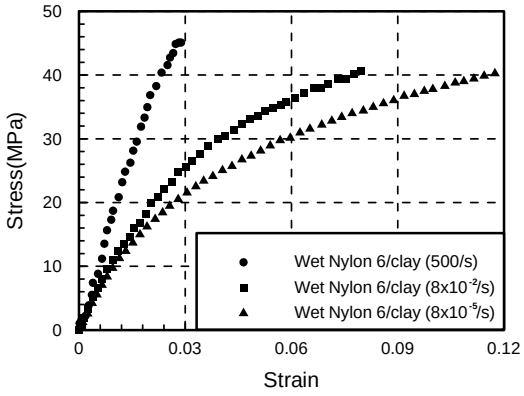

Figure 11. Stress and strain curves of wet nylon 6/clay nanocomposites at three different strain rates.

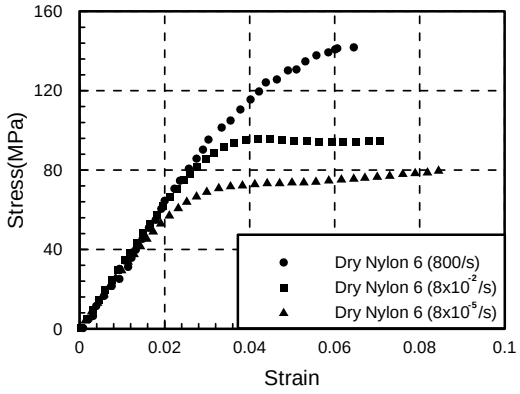

Figure 14. Stress and strain curves of unfilled dry nylon6 specimens at three different strain rates.

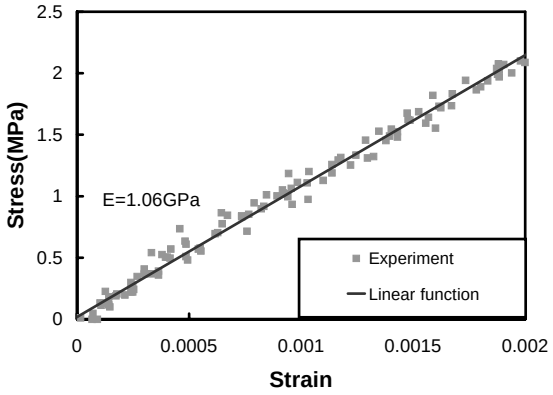

Figure 12. Determination of Young's modulus of wet nylon6/clay nanocomposites at strain rate of 0.00008/s.

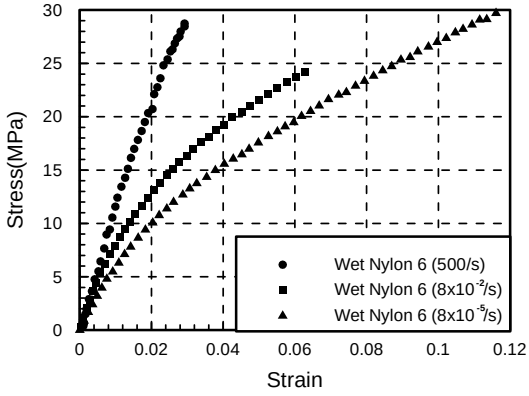

Figure 15. Stress and strain curves of unfilled wet nylon6 specimens at three different strain rates.

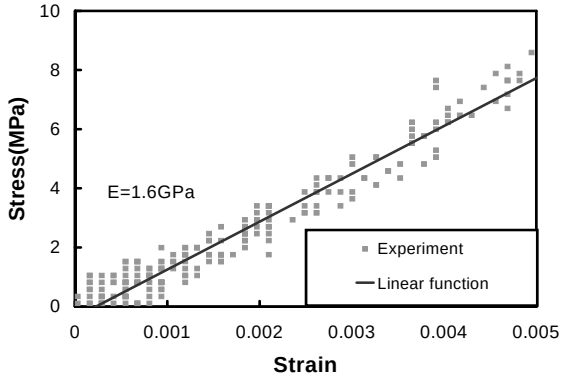

Figure 13. Determination of Young's modulus of wet nylon6/clay nanocomposites at strain rate of 500/s.